ISSN 0001-4370, Oceanology, 2016, Vol. 56, No. 2, pp. 214–225. © Pleiades Publishing, Inc., 2016.
Original Russian Text © M.V. Shokurov, V.A. Dulov, E.V. Skiba, V.E. Smolov, 2016, published in Okeanologiya, 2016, Vol. 56, No. 2, pp. 230–241.

MARINE PHYSICS

Wind Waves in the Coastal Zone of the Southern Crimea: Assessment of Simulation Quality Based on In Situ Measurements

M. V. Shokurov, V. A. Dulov, E. V. Skiba, and V. E. Smolov

Marine Hydrophysical Institute, Russian Academy of Sciences, ul. Kapitanskaya 2, Sevastopol

e-mail: shokurov.m@gmail.com

Received September 22, 2014; in final form, April 8, 2015

Abstract—The study verifies the Black Sea wave model using field data obtained from the Katsiveli research platform. The WAM and mesoscale MM5 and WRF atmospheric models, which are used to calculate the wind field for the wave model, were recently adjusted to the Black Sea region at the Marine Hydrophysical Institute. The results of the work are presented as characteristics of the simulation quality used in world practice in other regions. The scatter index for a significant wave height is 70% in summer and 50% in winter. The values of the scatter index of wave parameters and wind speed appear to be at the same level as in semi-enclosed seas on the northern side of the Mediterranean Sea. It is shown that atmospheric simulation correctly reproduces the interaction between synoptic processes and the mountain range extending alongshore. Error sources in wave simulation are discussed. The most significant drawback is the possibility of mesoscale instability in the atmospheric model without assimilation of observation data within the computational domain.

DOI: 10.1134/S0001437016020181

1. INTRODUCTION

In recent decades, significant progress has been made in simulating sea waves, which makes it possible to solve practical problems of wave prediction with a high degree of reliability; these can be used for safe navigation, application of shelf resources, assessment of wave climate and its trends, and the solution of scientific problems on meteorological wave phenomena using model simulations. These problems can be solved by using the results of global atmospheric simulation in mesoscale atmospheric and wave models, which need preliminary adjustment to a specific region. The MM5 and WRF mesoscale atmospheric models, together with the WAM wave model, which have been adjusted to the Black Sea region at the Marine Hydrophysical Institute in Sevastopol (before 2014, the Marine Hydrophysical Institute belonged to the National Academy of Sciences of Ukraine), are currently being used to assess the wave climate [2], short range meteorological and wave predictions [16], wave studies [15], and typical coastal atmospheric phenomena in the Black Sea [1]. Scientific aspects of the problem are the selection of correct parameterizations of natural processes in regional models, allowance for regional peculiarities [3, 7], and further verification of the models, which requires a specific validated approach.

The operational quality of wave models differs significantly if an open ocean or enclosed seas are considered. Traditionally, this is characterized by the scatter index *SI*, which is the ratio of the root-mean-square simulation error of a physical value to its mean observed value. The *SI* values for wind velocity, significant wave height, and period of the wave spectrum peak evaluated in the global forecast currently reach 15% [20]. However, over the scales of the Mediterranean Sea, the *SI* value increases up to 30–70% [8, 11, 12]. Since the vector field of wind velocity at a level of 10 m, which is the result of atmospheric simulation, is used as the input for the wave model, the quality of wave simulation is strongly determined by the quality of the atmospheric simulation. In particular, the wave characteristics in the northern part of the Mediterranean Sea are simulated worse than in its southern part owing to the existence of coastal mountainous terrain on the northern side, which is not adequately taken into account by atmospheric models [8, 11]. It is likely that targeted validation of the wave model in the Black Sea has not yet been performed. Our work attempts to make up for this disadvantage to some extent.

A standard approach to this problem implies that the data from three sources should be compared: the results of the model simulations, satellite data, and field records from meteorological and wave buoys [8, 12]. Usually, the fields of the wind and wave characteristics reconstructed from satellite data are calibrated using available field data [12]. This, in turn, makes possible the systematic comparison of the model and satellite fields in the entire studied basin. However, data from meteorological and wave buoys in the Black

Sea do not enjoy free public access. Therefore, strictly speaking, the reliability of the satellite data in the Black Sea (e.g., the known joint SeaWind dataset [22]) requires confirmation. In this work, the results of model simulations of wave characteristics are compared with field data from the Stationary Oceanographic Platform of the Experimental Department of the Marine Hydrophysical Institute in Katsiveli. Note that the waves observed at a specific point of the closed basin develop under wind forcing over the entire area of the basin. Therefore, comparison of the measured wave characteristics with simulated ones results in an indirect method for verification of atmospheric models and assessment of their "integral quality" related to the entire wind field over the sea. The aim of our work is to obtain such an assessment for the Black Sea in the form of characteristics used in similar assessments for the Mediterranean Sea and global model. We also show possible causes of the observed discrepancies.

2. DESCRIPTION OF DATA

2.1. Field Measurements

Field data were obtained at the Stationary Oceanographic Platform (33°59′ E, 44°23′ N) near the town of Katsiveli on the southern Crimea coast during three representative time periods: October 2012–April 2013, July–October 2012, and September–October 2011. The platform is located at a distance of 0.5 km from the shore over a depth of approximately 30 m. A mountainous plateau about 1000 m in elevation extends along the coastline approximately 4 km from the shore. The elevation gradually decreases between the plateau and the coast. The form of the platform, its location relative to the coastline, and a schematic section of the coastal zone topography normal to the coast are given in [5, 16,] and many other works.

The wind speed and direction were recorded at a height of 21 m with a time sampling of 1 min by the "Davis Vantage Pro 2" meteorological station installed on the platform. The wind velocity vectors averaged over 20-min intervals, whose centers corresponded to the time instant of the simulation point, were used for comparison with simulations.

Surface waves were recorded with a frequency of 10 Hz using an array of resistance wave recorders with string diameters of 0.25 mm. Each sensor measured the sea surface elevation with an error smaller than 1 cm, while wave heights were up to 4 m. Five strings were located at the vertices of a regular pentagon with a radius of 25 cm, and one was located at its center. This made it possible to determine the frequency and angular characteristics of waves with lengths ranging from 1.5 to 100 m. Perturbations introduced by the wave staffs to the measured wave field were minimized by an original suspension system. The entire construction was locked in place on a lifting support at a distance of 10 m from the closest pillar of the platform. The wave staff array was either lifted of lowered as a whole for direct calibration of the measuring recording system, while the values of its vertical displacements were measured exactly [6]. The design scheme of the system is described in [4]. A special design was applied for wave recording from October 2012 to April 2013, which consisted of one string wave recorder with increased strength characteristics, making it possible to record waves with heights up to 10 m. The technical details of the system were retained as described above, but the data were transmitted via radio channel to an onshore receiving device.

The wave data passed quality control, and unreliable fragments were filtered out [6]. Intervals of continuous records 1 h long were used to compare with simulations. The frequency and directional frequency spectra of sea surface elevations, $S(f)$ and $S(f,\vartheta)$ ($S(f) = \int d\vartheta S(f,\vartheta)$), were estimated for each of the intervals. Two-dimensional spectra were calculated using the maximum entropy method [17]. A significant wave height, the mean frequency and direction of the waves of the spectral peak,

$$H_S = 4\sigma, \quad \sigma^2 = \oint d\vartheta \int df S(f,\vartheta), \tag{1}$$

$$\bar{f} = \oint d\vartheta \int df \; fS(f,\vartheta)\big/\sigma^2, \tag{2}$$

$$\bar{\vartheta} = \arctan(b/a), \quad a = \oint d\vartheta \int df \cos(\vartheta) S(f,\vartheta), \quad b = \oint d\vartheta \int df \sin(\vartheta) S(f,\vartheta), \tag{3}$$

were determined from the spectra according to the definitions in [12], where σ^2 is the dispersion of the sea surface elevations. Although the values of the period and direction of waves of the spectral peak are traditionally used in comparison with field observations, several wave systems are frequently observed in our work both in the field data and simulated frequency-angular spectra, whose characteristics are difficult to compare. Therefore, below we restrict ourselves to comparison of the integral spectral characteristics $H_S, \bar{f}, \bar{\vartheta}$.

2.2. Simulation of the Atmosphere

We used the data of following types as the input to the wave model, which we obtained from atmospheric simulation over the Black Sea. The data are characterized by different spatial resolutions.

1. As the basis source we used the results of NCEP/NCAR global operational analysis, carried out by the US National Center of Atmospheric Research using all available data: land measurements, vertical profiles, satellite data, etc. The fields of atmospheric characteristics with a spatial resolution of 0.5° (appro-

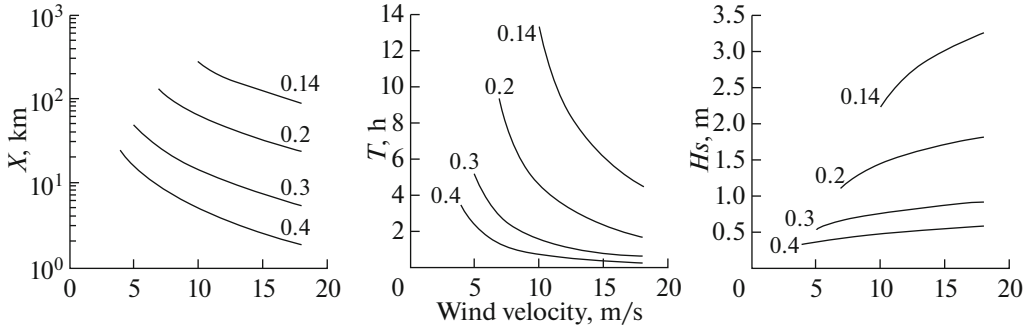

Fig. 1. Fetch (X), duration of wind action (T), and significant wave height (H_S) as functions of wind velocity. Numerals show frequency of spectral peak in Hz.

ximately 50 km) and time sampling of 6 h are free accessible on the Internet [13].

2. Wind velocity fields with a higher spatial resolution were obtained at the Marine Hydrophysical Institute using the MM5 mesoscale atmospheric model and its modern version Weather Research and Forecasting (WRF) [21]. The models were developed at the US National Center of Atmospheric Research, while at the Marine Hydrophysical Institute they were adjusted to the Black Sea region, by selecting the most appropriate schemes for parameterization of the physical processes and specifying in more detail the properties of the underlying surface and terrain topography, in particular [3]. The simulation domain covers the entire Black Sea basin (39°–49° N, 25°–45° E); the results of global active analysis are used as the lateral boundary conditions. We performed a retrospective analysis with a spatial resolution of 18 km and time sampling of 1 h using the MM5 model for the entire Black Sea region that covers the time interval 2000–2013.

3. Since 2007, the Marine Hydrophysical Institute has carried out operational weather forecasting in the Black Sea region using the MM5 model. The spatial resolution for the entire Black Sea region was 10 km, and the time sampling was 1 h. The prediction results are free accessible on the Internet [19]. The size of the computational domain is 39°–49° N, 25°–45° E, so it covers the entire Black Sea basin and makes it possible to analyze the synoptic situation and mesoscale peculiarities. The results of the NCEP/NCAR global operational forecast are used as the lateral boundary conditions [13]. Short-term meteorological prediction is currently being done at the Marine Hydrophysical Institute for the Azov and Black Sea regions simultaneously using two mesoscale atmospheric models, MM5 and WRF.

We use the NCEP/NCAR results of global analysis, reanalysis, and forecast of the Marine Hydrophysical Institute as the input data for the wave model; for brevity, we denote the corresponding data as 1, 2, and 3.

2.3. Wave Model for the Black Sea and Approach to Comparing Simulation and Measurement Data

We used the WAM (cycle 4) for wave simulation, which is currently used for forecasting and analysis of wind waves in the World Ocean and internal basins [14, 18]. The basis of the model is the equation for the wave action spectrum that describes the wave propagation in the presence of currents and takes into account the interaction between the wave components in a four-wave approximation. The right hand part of the equation is supplemented by the terms describing the wave generation by wind and their dissipation due to wave breaking. The WAM model is designed to calculate the directional frequency spectrum of waves with the dispersion relation for a finite sea depth [14].

The entire basin of the Black Sea was simulated over a regular grid with a step of 10 km. The time step providing stability of the numerical scheme was 5 min. The currents in the Black Sea were traditionally not taken into account because the available information about them is not sufficiently reliable. The fields of the wind velocity and direction at a height of 10 m were input to the WAM model from data of 1–3 types using linear spatial and temporal interpolations. The directional frequency spectrum $S(f,\vartheta)$ at the point of the simulation grid closest to the measurement point was used for comparison with measurements.

We selected the frequency range 0.04–0.4 Hz to calculate the spectra based on the following considerations. Figure 1 shows the semiempirical dependences of significant wave heights and periods of the spectral peak waves on the wave fetch and wind velocity. We used formulas [14], which take into account the fact that the wave spectrum tends to the limiting Pierson–Moskowitz spectrum in the course of wave development. The figure shows the curves at fixed frequencies of the spectral peak and the range of wind velocities of is interest to us. The figure for wave fetch means that waves should travel distance X to reach the indicated peak frequency at the given wind velocity. The duration of wave forcing on developing waves was estimated using the formula $T = X/C_G$, where C_G is the

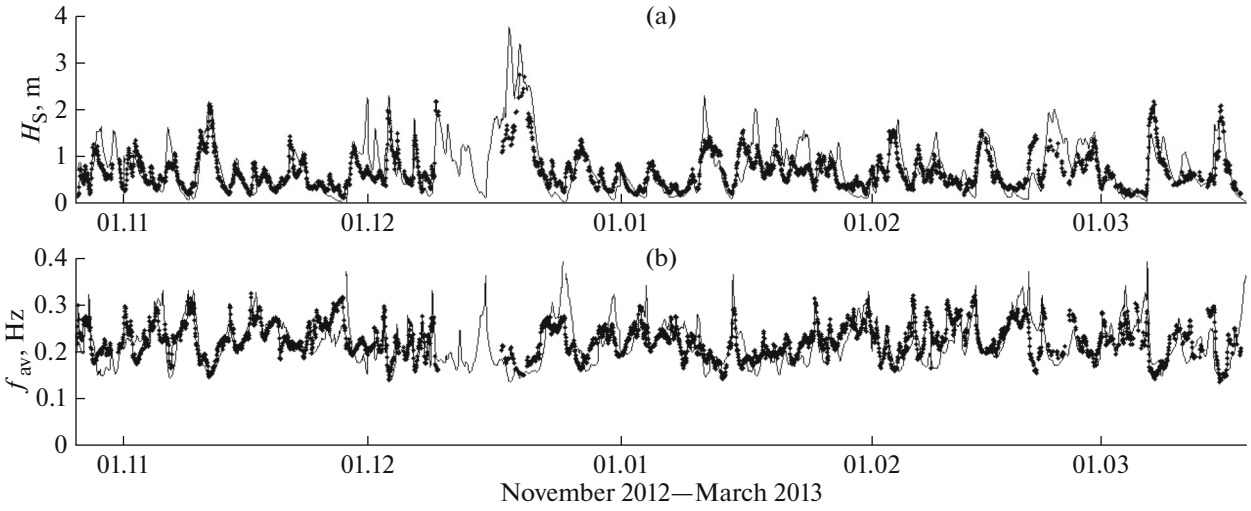

Fig. 2. Significant wave height (a) and mean wave frequency (b) in winter period of 2012–2013. Dots show field data; line shows simulation 3 (operational atmospheric forecast of Marine Hydrophysical Institute with resolution of 10 km).

group velocity of the spectral peak waves. The curves break down when wind velocity decreases and the indicated peak frequency cannot be reached, because it is lower than the limiting Pierson–Moskowitz spectral peak frequency. The graphs give us an idea about the values of wave characteristics that can be expected at the measurement point.

Wave spectra with frequencies within 0.15–0.3 Hz are usually observed at the Katsiveli platform. Swell usually exists when wind velocities are smaller than 3–5 m/s; hence the significant wave heights H_S remain at a level of 0.2–0.3 m or higher. It follows from the figure that a fetch of tens and hundreds of kilometers is needed for the development of such waves. Therefore, simulation of waves at the location of the platform requires simulation over the entire Black Sea basin. The figure also shows that wind conditions that influence the waves in Katsiveli have been achieved over the Black Sea in the period preceding the observations, which is several (up to 10) hours long. It is most likely that if the frequency of the wind wave peak in Katsiveli is 0.4 Hz or higher, the heights of such waves according to the figure for H_S will not exceed the contribution of the wave background related to the swell. On the basis of these considerations, the wave spectra were simulated for the region covering the entire Black Sea. The prognostic (simulated) frequency interval of the spectrum was limited to the maximum frequency of 0.4 Hz.

Note that, currently, simulation of the wave characteristic using nested grids became widespread [10], which makes it possible to account for the coastline in detail. In our case, when we limit the calculation to a maximum frequency of 0.4 Hz, such detailed elaboration makes no sense, because we take into account only the waves formed over an area greatly exceeding the characteristic distance between the platform and the coast. On the other hand, wave components with frequencies lower than 0.4 Hz can be present in the model spectrum, which arrive from directions actually located in the shadow zone formed by the details of the coastline. We consider only the spectra in the interval of wave arrival azimuths 45°–255° corresponding to the directions to the open sea so as to exclude these components from comparison with measurements. We emphasize that spectral peaks with frequencies lower than 0.4 Hz, which are in the excluded domain, are not present in the spectral estimates obtained from measurements.

Thus, in comparison to the observations, we use the wave characteristics determined from the spectra calculated using formulas (1)–(3), but integration in these formulas is performed over a frequency interval lower 0.4 Hz and an interval of wave arrival azimuths of 45°–255°.

3. RESULTS

Figure 2 makes it possible to compare the field data with model simulations using data 3. The figure shows the significant wave height and mean wave frequency calculated using formulas (1)–(2) for the winter season of 2012–2013. It follows from the plot that in calm periods, the value of H_S remains at a level of 20–30 cm, while the calculated values of H_S are sometimes one order of magnitude smaller. These situations correspond to the observations of weak swell in conditions when swell is not present in the model simulation. One can see sharp "peaks" at certain time instants in the plot of the mean wave frequency, where the calculated $\overline{f}$ is significantly higher than the measure one. The fact that the wave models do not describe well the decay of swell waves has been many times described in the literature; see, for example, [9]. Although the correct description of the waves in calm weather can hardly be

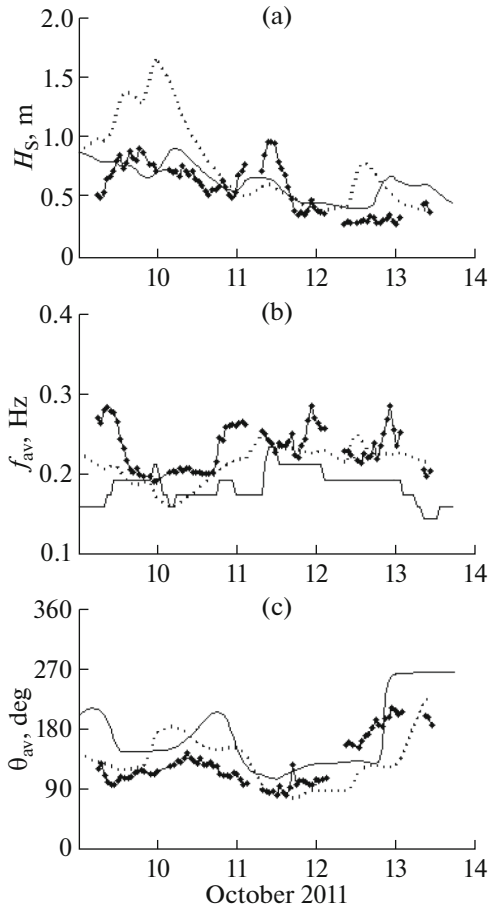

Fig. 3. Data fragment in October 2011. (a) Significant wave height, (b) mean wave frequency, (c) mean direction of waves. Dots show field data; solid line shows simulation 1 (NCEP/NCAR operational atmospheric analysis with resolution of 50 km); dashed line shows simulation 3 (operational atmospheric forecast of Marine Hydrophysical Institute with resolution of 10 km).

of practical importance, the mentioned discrepancies influence the statistical characteristics of the simulation quality.

Stormy conditions in the plot are distinguished from the peaks of significant wave heights. The calculated values of H_S near the peaks can be either lower (as in March 2013), or higher than the observed values. Such discrepancies can be as high as tens of percent. As we shall see later, the cause of such significant discrepancies is related to errors in simulations of wind speed in the atmospheric models. However, despite the mentioned causes, Fig. 2 demonstrates a clear correlation between the measured and calculated values. The abovementioned facts can be related to comparison of all simulations with all data.

Figure 3 shows a fragment of records in 2011. The figure demonstrates detailed time evolution of the data including mean wave direction (see formula (3)). Here, the geographical azimuth was taken as the wave direction from which the waves arrive (similar to the wind direction). Figure 3 also makes it possible to compare the results of the simulation based on data 1 and 3. On October 10, one can see an anomalously strong divergence of curves for H_S; we discuss this below. The deviations of H_S for the other dates, as also deviations of $\overline{f}$, and $\overline{\vartheta}$ shown in the figure are typical.

Figure 4 shows examples of the scatter diagrams for significant wave heights and mean frequency plotted by means of joining the data of all periods of measurements. The gray scale shows the relative frequencies of the points with given measured and calculated values. The diagrams illustrate the degree of correlation between the results of simulation and measurements. It follows from Fig. 4 that the simulation using data 1 underestimates the values of H_S, while the simulation using data 3 overestimates them. At the same time, the scatter diagrams for the medium values of wave frequencies are practically the same for the simulations with data 1 and 3.

Let us now characterize the degree of quantitative correspondence by calculating the following characteristics of simulation quality: bias

$$bias = \langle U_{\text{mod}} \rangle - \langle U_{\text{mes}} \rangle, \tag{4}$$

where U is a scalar value; subscripts $_{\text{mod}}$ and $_{\text{mes}}$ are related to the simulated and measured values, while the angular brackets denote averaging over a set of data; root-mean-square deviation

$$\text{RMSE} = \sqrt{\left\langle (U_{\text{mod}} - U_{\text{mes}})^2 \right\rangle}; \tag{5}$$

the linear regression coefficient *slope*, determined from equation

$$U_{\text{mod}} = slope \cdot U_{\text{mes}} \tag{6}$$

using the least square method; the scatter index according to two definitions

$$SI = \text{RMSE} / \langle U_{\text{mes}} \rangle$$
$$\text{and } SI2 = \sqrt{\left\langle (U_{\text{mod}} - slope\, U_{\text{mes}})^2 \right\rangle} \Big/ \sqrt{\left\langle U_{\text{mes}}^2 \right\rangle}; \tag{7}$$

the correlation coefficient

$$r = \left\langle (U_{\text{mod}} - \langle U_{\text{mod}} \rangle)(U_{\text{mes}} - \langle U_{\text{mes}} \rangle) \right\rangle \Big/ \sqrt{\left\langle (U_{\text{mod}} - \langle U_{\text{mod}} \rangle)^2 \right\rangle \left\langle (U_{\text{mes}} - \langle U_{\text{mes}} \rangle)^2 \right\rangle}. \tag{8}$$

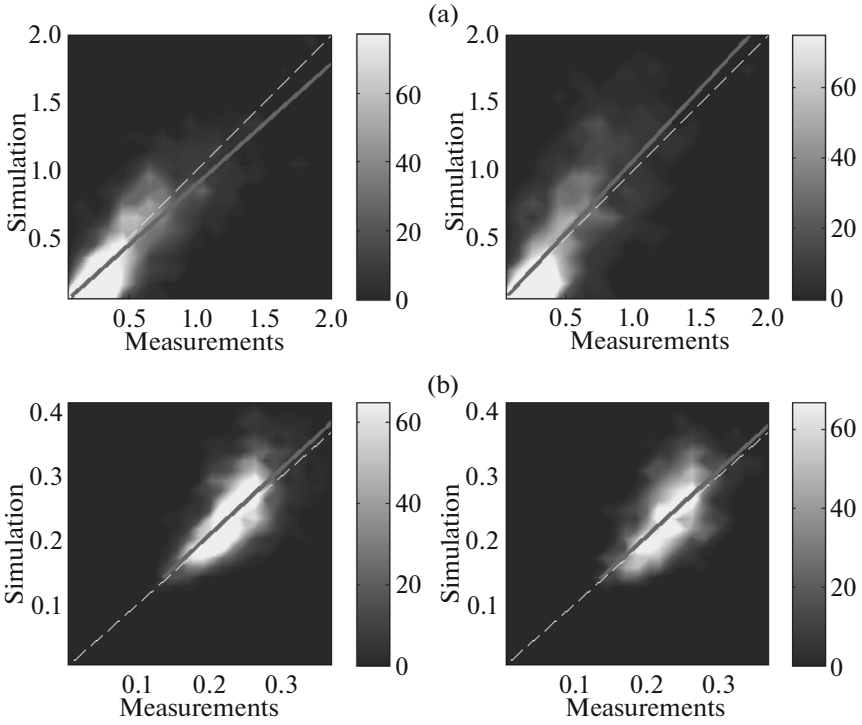

Fig. 4. Scatter diagrams of wave characteristics. (a) significant wave height, (b) mean wave frequency. Comparison with simulation 1 is shown on left (NCEP/ NCAR operational atmospheric analysis with a resolution of 50 km), comparison with simulation 3 is shown on right (operational atmospheric forecast of Marine Hydrophysical Institute with resolution of 10 km). Dashed straight line shows complete correspondence; solid straight line shows result of linear regression.

We characterize the quality of simulations of wave direction by the bias of the mean direction and standard error deviation:

$$bias_{\text{dir}} = \langle \vartheta_{\text{mod}} \rangle - \langle \vartheta_{\text{mes}} \rangle$$
$$\text{and } SDE_{\text{dir}} = \sqrt{\left\langle \left(\vartheta_{\text{mod}} - \vartheta_{\text{mes}} - bias_{\text{dir}} \right)^2 \right\rangle}, \quad (9)$$

where the mean angles were calculated by averaging of $\exp(i\alpha)$ similar to (3). It is likely that cases of small significant wave height (for example, $H_S < 0.3 - 0.5$ m) are not very interesting for estimating the quality of wave direction calculation. We carry out averaging in formulas (9) with a weight proportional to the significant wave height to suppress their contribution. Let us calculate these characteristics for the entire data set and for the three-month-long periods of June 15, 2012–September 15, 2012 (summer) and December 1, 2012–March 1, 2013 (winter). Table 1 gives the corresponding mean values of the measured significant wave heights and mean wave frequency, and the coefficients of their variations determined as the ratio of the standard deviation to the mean value.

Table 2 presents the characteristics of the simulation quality of significant wave heights, mean wave frequency, and mean wave direction based on simulations 1–3 from the joint data set. Table 2 also includes two columns showing the divergence between the two model simulations. Here, column "2 and 1" means that during the simulations using formulas (4)–(9), data 1 were substituted from the measured values, which are compared with data 2; column 3 and 1 has a similar sense. These columns compared with the first three columns of the tables show that the divergences between the results of simulations and measurements are not much greater than the divergences between simulations. Table 3 makes it possible to compare the simulation quality in the summer and winter seasons.

It follows from the table that the scatter index for H_S is at a level of 40–60%, which is determined worse than wave simulation in the open ocean [20]. However, these values correspond to the scatter indices in the coastal zone on the northern side of the Mediterranean Sea (25–70% as reported in [8, 12]).

Table 1. Mean characteristics of field data

Characteristics of data	Entire data set	Summer	Winter
$\langle H_S \rangle$, m	0.52	0.39	0.67
$k_{\text{var}}(H_S)$, %	64	60	55
$\langle \bar{f} \rangle$, Hz	0.24	0.25	0.22
$k_{\text{var}}(\bar{f})$, %	15	13	15

Table 2. Characteristics of simulation quality over entire data set

Parameter	Characteristics of quality	Number of simulation			Comparison of simulations	
		1	2	3	2 and 1	3 and 1
H_S	*bias*, m	–0.0579	0.0522	0.0270	0.1152	0.0851
	RMSE, m	0.2101	0.3291	0.3091	0.2498	0.2223
	SI, %	40.5724	62.5780	59.7795	53.7660	48.2459
	SI2, %	33.8285	52.3287	49.8784	40.9492	35.9888
	slope	0.8963	1.0979	1.0730	1.2073	1.1815
	r	0.8260	0.7502	0.7738	0.8705	0.8984
$\overline{f}$	*bias*, Hz	0.0097	0.0057	0.0071	–0.0042	–0.0020
	RMSE, Hz	0.0395	0.0430	0.0426	0.0336	0.0284
	SI, %	16.4467	17.9395	17.7540	13.5036	11.4264
	SI_2, %	16.3061	17.7776	17.5982	13.0344	11.1343
	slope	1.0378	1.0177	1.0256	0.9743	0.9871
	r	0.6555	0.5701	0.6016	0.7907	0.8512
$\overline{\vartheta}$	$bias_{\mathrm{dir}}$, °	14.2216	3.8878	7.5029	–7.4019	–5.6345
	SDE_{dir}, °	35.2711	39.8423	40.4287	38.0324	34.7409

Table 3. Characteristics of simulation quality in summer and winter periods

Parameter	Characteristics of quality	Summer, data type			Winter, data type		
		1	2	3	1	2	3
H_S	*bias*, m	–0.0680	0.0391	–0.0027	–0.0591	0.1094	0.0732
	RMSE, m	0.1967	0.3266	0.2878	0.2187	0.3491	0.3798
	SI_1, %	50.0048	83.0066	73.1503	32.4322	51.7596	56.2202
	SI_2, %	43.6228	70.0091	62.0261	28.0619	45.2316	48.8693
	Slope	0.8854	1.1488	1.0688	0.9092	1.1485	1.1181
	r	0.7829	0.6889	0.7329	0.8377	0.7598	0.7481
$\overline{f}$	*bias*, m	0.0198	0.0139	0.0219	0.0006	–0.0047	–0.0026
	RMSE, m	0.0475	0.0496	0.0508	0.0299	0.0385	0.0380
	SI_1, %	18.7043	19.5068	20.0171	13.3730	17.2244	17.0248
	SI_2, %	18.7815	19.5895	20.1754	13.2131	16.9232	16.7800
	Slope	1.0714	1.0439	1.0776	0.9990	0.9730	0.9839
	r	0.4153	0.2423	0.3228	0.7087	0.5568	0.5921
$\overline{\vartheta}$	$bias_{\mathrm{dir}}$, °	10.3160	–1.4992	2.0814	–	–	–
	SDE_{dir}, °	34.1436	36.3131	38.5470	–	–	–

All simulations show that the bias of H_S appears at a level of a few centimeters; the bias of $\overline{f}$ is at a level of 0.01 Hz or lower; the bias of $\overline{\vartheta}$ is at a level of 10° or lower. The values of *slope* for H_S show that the simulations based on data 1 always underestimate the wave heights, whereas simulations with data 2 and 3 overestimate this value. The values of *slope* for $\overline{f}$ show that all simulations overestimate the mean wave frequency in summer and underestimate it in winter. Judging from the values of scatter indices *SI* and *SI*2, the mean wave frequency is modeled with a better quality than the significant wave height; in addition, H_S and $\overline{f}$ in the winter season are modeled better than in the summer season. We note that correlation coefficient *r* for $\overline{f}$ is always lower than for H_S, which can be related to insufficiently adequate description of swell in the wave model. The mean wave direction is modeled with a significant error at a level of 40° (see line SDE_{dir} in the

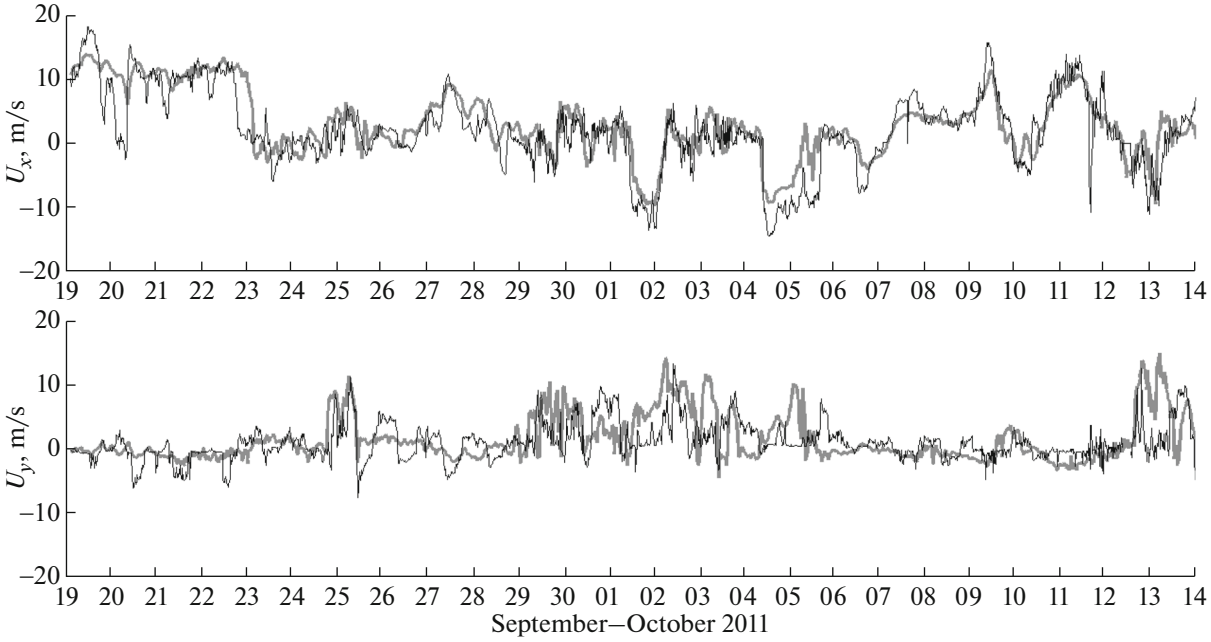

Fig. 5. Wind velocity components along ridge (U_x) and normal to ridge (U_y). Black line shows field measurements; thick gray line shows simulation 5 (WRF model with resolution of 3 km).

tables). Note that the divergences between the values of $\overline{\vartheta}$ in different simulations are at the same level (see Table 2).

It is seen from Tables 2 and 3 that the coefficient of correlation between the measured and modeled wind wave parameters decreases systematically (although insignificantly) with increasing resolution of the atmospheric model used for simulation of wind fields. The same can be said about the RSME scatter values. Below, we consider the possible causes of these divergences between the measurement data and simulation results. First of all, we have to assess the simulation quality of wind fields used as the input data for the wave model.

4. SIMULATION OF THE ATMOSPHERE AS A POSSIBLE SOURCE OF DISCREPANCY

The available data make it possible to directly compare wind velocity simulations with field measurements from the Katsiveli platform. However, owing to the fact that the platform is located in the coastal zone, it is desirable to use simulations with increased spatial resolution for comparison. Such simulations were specially performed using the WRF model in the measurement period of September–October 2011. The reanalysis data with a resolution of 18 km (simulation 2) were used as the boundary conditions for downscaling in three nested domains with a center at the location point of the platform [7]. The domains were squares with sides of 829, 276, and 93 km, and the grid steps were 9, 3, and 1 km. For brevity, we denote these simulations as 4, 5, and 6, respectively. Thus, six types of data with spatial resolutions of approximately 50, 18, 10, 9, 3, and 1 km were available for analysis. The results of these simulations at the nodes of a vertical grid at a height of 20 m, which is the closest to the measurement height (21 m), were used for comparison with measurements.

The simulation should a priori correctly describe the synoptic variability of the atmospheric fields owing to application of the nested grid method when detailed structure in the given region is simulated for known large-scale fields (data 1). Therefore, the results of simulations should demonstrate the interaction of synoptic processes with the main peculiarity of the underlying surface topography, with the mountain ridge extending along the coast. Figure 5 shows the wind velocity components along the ridge (U_x) and normal to the ridge (U_y) according to measurements and simulation 5. An azimuth of 65° was selected as the general direction of the ridge; the eastern direction corresponds to positive U_x values, and the northern direction corresponds to positive U_y values.

The wind flow in this period was generally directed along the ridge. It was characterized by variations over scales of a few days. These main features of the wind field are well described by the model. However, variations on the scale of one day or less are worse reproduced, especially the wind component normal to the ridge. For example, in the period from September 25 to 29, one can distinguish fluctuations of U_y with approximately a daily period, which the simulations do not reproduce. However, simulation describes a

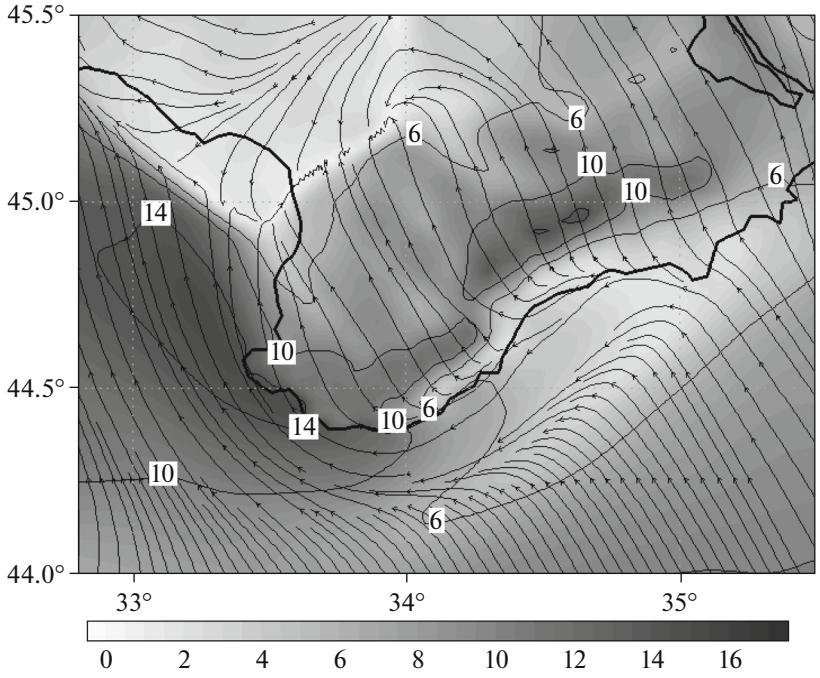

Fig. 6. Alongshore jet on October 9, 2011, at 12:00 UTC. Wind field is shown in grayscale and directed streamlines. Coordinate axes are northern latitude and eastern longitude. Numerals on grayscale and contour lines show wind velocity in m/s. Black line shows land–sea boundary.

number of characteristic regional effects. For example, in the period from September 24 to 26, the wind over the entire Black Sea was northerly. During such a synoptic situation, the wind velocity over the Katsiveli platform can be either very small when the platform is in the wind shadow zone or, on the contrary, the velocity can be high during the slope wind with local intensification at the foot of the ridge. One can see in Fig. 5 that the wind in this period was weak, but in a period of a few hours (night–morning on September 25) the wind sharply intensified. The model reproduces this situation well.

The model describes a specific phenomenon of this region: formation of an alongshore jet when the wind flows around the Crimean Mountains. Figure 6 shows an example of the jet on October 9, 2011, at 12:00 UTC (simulation 5). The jet is well seen in Fig. 5, which shows the measurements of alongshore wind component U_x. It is manifested as an intensification of wind velocity up to 12–15 m/s in a narrow coastal zone approximately 30 km wide.

Detailed simulations of wind velocity cover a period of 28 days. Table 4 shows the characteristics of the quality for this simulation and wind directions for all types of the model data calculated from formulas (4–9). All the wind direction characteristics in formulas (9) were averaged with a weight proportional to the wind velocity. The mean measured wind velocity is 6.10 m/s, and its variation coefficient is 62%.

Note that the estimate for the scatter index of wind velocity in Table 4 is at the same level as for the atmosphere simulation in semienclosed seas on the northern side of the Mediterranean Sea [8]. Comparison of Table 4 with Tables 2 and 3 shows that the quality of wind velocity and direction simulation is no better than the quality of simulation of significant wave height and mean direction of waves. This supports the conclusion that atmosphere simulation is an important, and possibly, the main source of errors in the simulation of wave fields.

It was concluded in [16] that the two strongest weather disasters in the Black Sea region in recent years were predicted by the forecast of the Marine Hydrophysical Institute (simulation 3 with a resolution of 10 km), but they were not predicted by the global NCEP/NCAR forecast (data 1 with a resolution of 50 km). It was shown in [11, 12] that the simulation quality of wind and waves in the Mediterranean Sea increases with increasing spatial resolution of the models. The quality of wind field simulation in the region of the southern coast of Crimea also increases with increasing resolution of the models; for example, the alongshore jet shown in Fig. 6 is clearly pronounced in the fields of the model wind velocity with resolutions of 1 and 3 km (simulations 6 and 5), but it is not present in simulations with a worse resolution. However, it follows from Table 4 that the characteristics of the quality of wind velocity simulation at the point of the platform actually were independent of the

Table 4. Characteristics of simulation quality of wind velocity and direction

Characteristics	Data type					
	1	2	3	4	5	6
bias, m/s	−1.7298	−0.7824	−0.0433	−2.0618	−0.7347	−0.1957
RMSE, m/s	3.1676	3.5874	3.4283	2.8498	3.1634	3.4411
SI, %	54.6242	61.0368	58.3311	48.5027	51.8024	58.5673
*SI*2, %	23.8158	38.0912	40.0862	26.5534	39.2431	46.1471
Slope	0.5630	0.6793	0.7842	0.5790	0.7893	0.8584
r	0.6736	0.4124	0.4821	0.6721	0.6170	0.6007
$bias_{dir}$, °	5.7967	11.1342	15.8910	10.4986	11.3211	11.4869
SDE_{dir}, °	46.3734	58.1434	51.3671	43.1418	41.1899	51.2616

resolution. The authors of [8] also faced a similar situation. According to their interpretation, random motions appear with increasing resolution of the model, which add energy into the small-scale part of the spectrum of wind velocity variations and lead to intensification in the scatter of points in the scatter diagram.

Analysis of our results also reveals another possible cause of divergence: "atmospheric model instability" without data assimilation within the computational domain. Figure 7 shows the wind fields over the Black Sea corresponding to two types of simulations for 12:00 UTC on October 9, 2011. The simulations result in two qualitatively different situations. Simulation 3 (spatial resolution is 10 km) results in propagation of a mesoscale atmospheric front over the sea, whereas the result of the global model demonstrates a field with low gradients. Let us consider the corresponding effect for the wave heights at the platform over 12 h (a time shift is needed to take into account wave development over the scale of the entire basin, see Fig. 1). A significant excess of the simulated significant wave height based on the wind field of type 3 over the measured values is seen in Fig. 3 close to 12:00 UTC on October 9, 2011. At the same time, the results of simulation 1 correspond to the measurements. Thus, there was actually no sharp front with wind velocities over 14 m/s in the warm sector before the front that results from simulation 3. It is likely that the actual front was much less pronounced. Modification and even generation of mesoscale atmospheric phenomena in the regional models within the domain of simulations with boundary conditions specified at the domain boundaries is a well-known peculiarity. If there is no data assimilation within the simulation domain, the model can result in strong divergence from the real state of the atmosphere. Currently, there are not enough available measurements with high spatial resolution for data assimilation using the mesoscale model. It is likely that such types of modification are infrequent: in our simulations, there was only one event in 28 days. However, this event

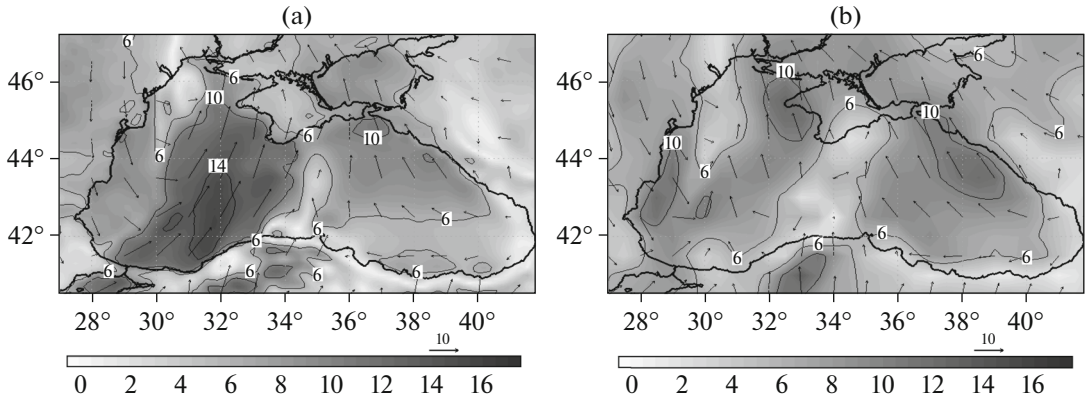

Fig. 7. Wind field at height of 20 m on October 9, 2011, at 12:00 UTC. (a) Simulation 3 (operational atmospheric forecast of Marine Hydrophysical Institute with resolution of 10 km), (b) simulation 1 (NCEP/ NCAR operational atmospheric analysis with resolution of 50 km). Notations same as in Fig. 6.

caused significant errors in wave height simulation. Therefore, it is of practical importance to find a way to avoid such errors.

5. CONCLUSIONS

We obtained an assessment of the simulation quality of wave fields in the Black Sea by comparison with field measurements from the Stationary Oceanographic Platform in Katsiveli. We used the WAM model (cycle 4) and the wind velocity fields in the Azov–Black Sea region obtained using the MM5 and WRF mesoscale atmospheric models. These models were adjusted to the region at the Marine Hydrophysical Institute. Since the development of waves observed at the platform occurs over the entire area of the basin, the obtained estimates characterize the "integral simulation quality" of waves in the Black Sea and in the atmosphere over the sea. We present a theoretical justification for the selection of the maximum frequency of 0.4 Hz when simulating wind waves in the Black Sea. Correct comparison with measurements at the point of the platform requires that the angular range corresponding to the directions of wave development from the coast (255°–45°) should be excluded from the simulated spectrum. Special simulations of the atmospheric fields with increased spatial resolution (up to 1 km) using the nested grid method were performed to analyze the wind fields in detail. The results are presented as the simulation quality characteristics used in world practice in other regions (see Tables 2–4).

The results show that the simulation quality of significant wave heights and wind velocity in the coastal zone of the southern coast of Crimea, characterized by scatter indices within 40–60%, correspond to semienclosed seas on the northern side of the Mediterranean Sea, where the scatter index can be as high as 70% [8, 12]. The simulation quality of the mean wave frequency is higher: it approaches the results of global simulation ($SI \sim 15\%$). Simulation of the mean wave directions is less reliable (the characteristic error is at a level of 40°). In the winter season, wave characteristics are simulated more reliably than in the summer season (see Table 3), so that the scatter index for the significant wave heights in winter is 20% lower than in summer. Usually, swell with significant wave heights that do not exceed 0.5 m is observed in weak wind conditions, which is lacking in simulations. This (which may not be important from the practical viewpoint) indicates that swell decay in the wave model is inadequate.

The simulation quality of wind velocity does not exceed the simulation quality of wave characteristics (cf. Tables 2 and 4); thus, the atmospheric model may be the main cause of errors in the simulation of wave fields. Detailed comparison of the simulated wind velocity with the measurement data shows that the atmospheric model with increased spatial resolution (1–3 km) describes qualitatively correctly the interaction between the synoptic processes and the mountain ridge extending along the shore, reproducing alongshore jets, wind shadows, and sloping wind. At the same time, we revealed the drawbacks of the model, which can be divided into three types. First, the model poorly reflects wind velocity variations on time scales of one day or shorter, especially for the wind component normal to the ridge (see Fig. 5, plot U_y). Second, nondeterministic motions exist (found earlier in [8]), which appear when the model resolution increases. As a result, increased resolution does not lead to improvement in the characteristics of simulation quality of wind velocity and waves (see Tables 4 and 2). Third, there may be a situation of "model instability" in the simulation of the atmosphere, which may occur due to lack of data assimilation within the simulation domain (see Fig. 7). This leads to significant errors in wave height simulations. Currently, the third disadvantage is the most significant and its elimination is considered the most important problem in improving the regional atmospheric model at the Marine Hydrophysical Institute.

ACKNOWLEDGMENTS

The authors thank F. Ardhuin (Ifremer, France) for helpful discussions of the results.

The research was performed at the Marine Hydrophysical Institute, supported by the Ministry of Education and Science of the Russian Federation within the Federal Target Project "Investigations and Developments in Priority Fields for Development of the Scientific and Technological Complex of Russia in 2014–2020" (unique identifier RFMEFI57714X0110). The research was also supported by the Project "Towards COast to Coast NETworks of Marine Protected Areas Coupled with Sea-Based Wind Energy Potential (COCONET)" of the seventh framework EC Program (grant no. 287844, FP7/2007–2013).

REFERENCES

1. V. V. Efimov and V. S. Barabanov, "Breeze circulation in the black-sea region," Phys. Oceanogr. **19** (5), 289–300 (2009).
2. V. V. Efimov and O. I. Komarovskaya, *Atlas of Extreme Wind Waving in the Black Sea* (EKOSI-Gidrofizika, Sevastopol, 2009) [in Russian].
3. V. V. Efimov, S. V. Stanichnyi, M. V. Shokurov, and D. A. Yarovaya, "Observations of a quasi-tropical cyclone over the Black Sea," Russ. Meteorol. Hydrol. **33** (4), 233–239 (2008).
4. V. V. Malinovskii, V. A. Dulov, A. N. Bol'shakov, et al., "Methodological and technical support for adjustment of *Sich-1m* apparatus for analysis under marine surface: possible approach," in *Ecological Safety of Coastal and Self Zones, and Complex Use of Shelf Resources* (EKOSI-Gidrofizika, Sevastopol, 2004), No. 11, pp. 236–251.
5. Yu. P. Solov'ev, "Characteristics of internal boundary layer above sea winded from the mountainous coast," in *Ecological Safety of Coastal and Self Zones, and Complex*

Use of Shelf Resources (EKOSI-Gidrofizika, Sevastopol, 2010), No. 21, pp. 74–87.

6. E. V. Chechina, "Database of the wind-geographic data obtained from the Stationary oceanographic platform in Katsiveli of Experimental department of the Marine Hydrophysical Research Institute, National Academy of Sciences of Ukraine, in *Ecological Safety of Coastal and Self Zones, and Complex Use of Shelf Resources* (EKOSI-Gidrofizika, Sevastopol, 2013), No. 27, pp. 215–220
7. M. V. Shokurov, S. Yu. Artamonov, and I. N. Ezau, "Digital modeling of atmosphere in the region of Katsiveli platform for planning and interpretation of natural experiments," in *Ecological Safety of Coastal and Self Zones, and Complex Use of Shelf Resources* (EKOSI-Gidrofizika, Sevastopol, 2010), No. 21, pp. 239–251.
8. F. Ardhuin, L. Bertotti, J. R. Bidlot, et al., "Comparison of wind and wave measurements and models in the Western Mediterranean Sea," Ocean Eng., No. 34 (3), 526–541 (2007).
9. F. Ardhuin, B. Chapron, and F. Collard, "Observation of swell dissipation across oceans," Geophys. Res. Lett., No. 36, **L06607** (2009). doi 10.1029/2008GL037030
10. F. Ardhuin and A. Roland, "The development of spectral wave models: coastal and coupled aspects," in *Proceedings of Coastal Dynamics 2013: 7th International Conference on Coastal Dynamics* (University of Bordeaux, Bordeaux, France, 2013), pp. 25–38.
11. L. Cavaleri and L. Bertotti, "The accuracy of modeled wind and waves fields in enclosed seas," Tellus A, No. 56, 167–175 (2004).
12. L. Cavaleri and M. Sclavo, "The calibration of wind and wave model data in the Mediterranean Sea," Coastal Eng., No. 53, 613–627 (2006).
13. Environmental Modeling Center Global Forecast System, National Weather Service, NOAA, USA, 2014. http://www.emc.ncep.noaa.gov/index.php?branch=GFS
14. L. H. Holthuijsen, *Waves in Oceanic and Coastal Waters* (Cambridge University Press, 2007).
15. V. A. Ivanov, V. A. Dulov, S. Yu. Kuznetsov, et al., "Risk assessment of encountering killer waves in the Black Sea," Geogr., Environ., Sustainability, No. 1, 84–111 (2012).
16. V. A. Ivanov, M. V. Shokurov, V. A. Dulov, et al., "Operational atmospheric modeling for advance warning of weather disasters in the Black Sea region," Geogr., Environ., Sustainability **6** (4), 31–47 (2013).
17. K. Kahma, D. Hauser, H. E. Krogstad, et al., *Measuring and Analyzing the Directional Spectra of Ocean Waves, EU COST Action 714. EUR 21367* (Brussels, 2005).
18. G. J. Komen, L. Cavaleri, M. Donelan, et al., *Dynamics and Modeling of Ocean Waves* (Cambridge University Press, Cambridge, UK, 1994).
19. *Marine Hydrophysical Institute 5-Day Weather Forecast over the Black Sea* (Atmosphere-Ocean Interaction Department, Marine Hydrophysical Institute, Sevastopol, 2014). http://vao.hydrophys.org
20. D. S. Richardson, "Verification statistics and evaluations of ECMWF forecasts in 2011–2012," in *ECMWF Technical Memoranda* (European Centre for Medium Range Weather Forecasts, Shinfield Park, UK, 2012), No. 688. http://www.ecmwf.int/publications/
21. W. C. Skamarock, *A Description of the Advanced Research WRF Version 3. NCAR Technical Note NCAR/TN-475+STR* (Mesoscale and Microscale Meteorology Division, National Center for Atmospheric Research, Boulder, CO, 2008).
22. H.-M. Zhang, J. J. Bates, and R. W. Reynolds, "Assessment of composite global sampling: sea surface wind speed," Geophys. Res. Lett., No. 33, **L17714** (2006). doi 10.1029/2006GL027086

Translated by E. Morozov